Journal of Physics: Conference Series

PAPER • OPEN ACCESS

Energetic comparison between different configurations of a concentric magnetic gearbox for industrial applications

To cite this article: Amedeo Amoresano *et al* 2024 *J. Phys.: Conf. Ser.* **2893** 012035

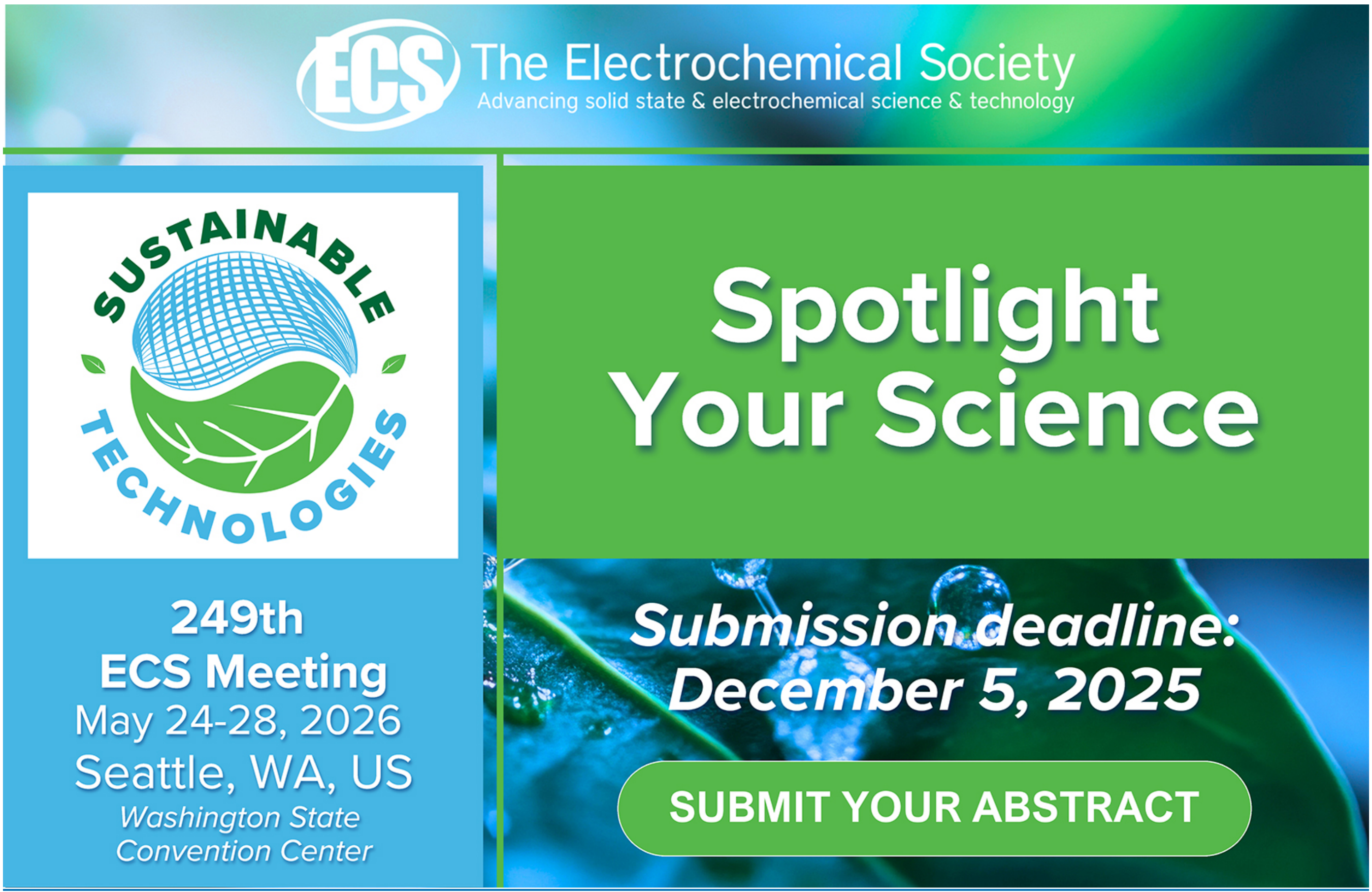

Journal of Physics: Conference Series **2893** (2024) 012035 doi:10.1088/1742-6596/2893/1/012035

Energetic comparison between different configurations of a concentric magnetic gearbox for industrial applications

Amedeo Amoresano[1*], Silvia Roscioli[1], Giuseppe Langella[1], Paolo Iodice[1]

[1] Industrial Engineering Department, University of Naples 'Federico II', 80125, Naples, Italy

*E-mail: amedeo.amoresano@unina.it

Abstract. Mechanical gearboxes can achieve high torque densities. They often require recurring lubrication, cooling and maintenance, and reliability can be a significant issue, particularly for remote systems such as wind turbines, or during the operation of a ship under special conditions or circumstances that require an immediate response. For these reasons, a new type of gearbox is increasingly gaining ground, namely magnetic gearboxes (MG). It operates without contact between the moving parts and consists mainly of three concentric 'rings' with a number of permanent magnets and iron poles to achieve a specific gear ratio. This article presents an energy comparison in terms of induced torque between different configurations of a concentric magnetic gearbox in terms of material construction for the cores, magnets position and number of pole pairs. The data were realised using the two-dimensional Finite Element Method (FEM). The results show that although the polymer-based configuration shows some potential, the ferrous core with external magnets significantly outperforms it in terms of torque and efficiency.

1. Introduction

Nowadays, the reduction of fossil fuels coupled with the mitigation of greenhouse gas emissions constitutes a crucial topic in research related to renewable energy sources [1]. Specifically, industries, such as those producing small wind turbines and solar panels, aim to adopt wind and solar power to accomplish the previously mentioned goals [2],[3]. In industrial applications linked to wind turbines, gearboxes constitute fundamental components capable of conveying the energy produced by the wind into the generator with suitable velocity. The gearboxes typically used for wind turbines are mechanical ones [4], making some disadvantages such as noise sources, malfunctions due to structural overloads [5]-[7] and ice accretion [8], and they require scheduled maintenance operations. Therefore, consequences, which include imbalanced shafts, leaking oil, excessive heating, and inadequate lubrication [9], are linked to the previously described disadvantages due to adopting traditional mechanical gearboxes. A reliable alternative to mechanical gearboxes is constituted by Magnetic Gearboxes (MGs), in which the contact between gears is cancelled by adopting rotating magnetic gears. Therefore, maintenance operations and acoustic noises are reduced [4],[10]-[13]. The typical topologies of MGs are concentric, harmonic and planetary [14],[15]. The reduction of noises and vibrations coupled with that linked to friction losses between mechanical parts can be achieved by determining the correct non-contact transmission of the torque between the input and output of gears based on

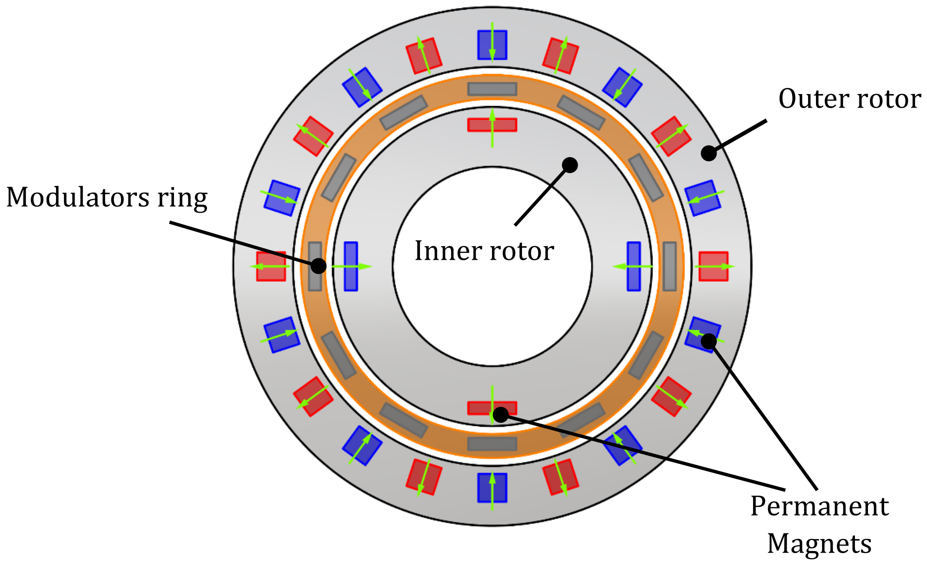

Figure 1. Coaxial MG scheme

the performance of the magnetic gears. A coaxial magnetic gear is composed of an inner rotor, outer rotor and a middle ring containing ferromagnetic parts (Figure 1). The coupling of different spatial harmonics between rotors and rings can be achieved by choosing the correct number of pole pairs related to the inner/outer rotor and the number of ferromagnetic parts included in the middle rings. In this way, different gear ratios can be obtained. The following gear ratios are obtainable considering a co-axial gear:

$$\begin{cases} \omega_{r,o}/\omega_{r,m} = p_m/p_o \\ \omega_{r,i}/\omega_{r,m} = p_m/p_i \\ \omega_{r,i}/\omega_{r,o} = -p_o/p_i \end{cases} \tag{1}$$

where $\omega_{r,o}$, $\omega_{r,i}$, $\omega_{r,m}$ are the angular speeds of the outer rotor, inner rotor, and middle rings of the gears, respectively. The $p_m = p_o + p_i$, p_o, and p_i are the number of ferromagnetic parts in the middle ring, the pole pairs in the outer rotor, and the pole pair in the inner rotors [16]. Due to the possibility of employing MGs for industrial applications, an energy comparison based on considerations related to the magnetic field generated in different configurations of a concentric three-ring magnetic gearbox is proposed in the present work. By considering the possibility of fixing one of the rings constituting the gearbox, the gear ratio, the values related to the torque and harmonic order amplitudes belonging to the magnetic flux density can be modified. Data adopted for the analysis are obtained by a two-dimensional model developed through the Finite Element Method (FEM) technique. Furthermore, different operating configurations related to the gearbox are explored in the present work by varying the dimension of the radius belonging to the external ring, the material employed for the support of magnets, and the layout of magnets positioned externally to the iron core.

2. Numerical Analysis

The numerical analysis employed was based on the Finite Element Method (FEM). Each model was divided into a mesh, comprising 26368 elements and 13424 nodes for the smaller models, and up to approximately 121958 elements with 61344 nodes for the larger models.

The objective of each individual FEM analysis was to evaluate the torque acting on each ring as the position of one ring varied. This approach allows for the assessment of the torque experienced by the remaining rings, based on the action-reaction principle, due solely to their presence in a rotating magnetic field under specific conditions.

The FEM analyses were conducted under various system configurations, both geometrically and technologically. The results were subsequently compared for each case. Comparisons were made for the unloaded system and across four varying parameters: *i)* the radius of the outer ring, *ii)* the material used for the rings, *iii)* the position of the magnets, and *iv)* the number of magnets used while maintaining the same transmission ratio. Specifically, the logic used for the comparison is shown in Table 1. In all simulations, a ratio of 1:5 between the number of pole pairs of the inner and outer rings was considered. As mentioned, the number of modulators is given by the sum of the pole pairs of the inner and outer rotors. Therefore, it is 12 for the first three comparisons and 24 for the last one.

Table 1. Comparisons made by varying the outer radius, magnet position, core material, and the number of pole pairs in the inner ring (p_i) and the outer ring (p_o). The benchmark terms are indicated in bold.

ID configuration	External Radius	Magnets position	Core material	p_i/p_o
1	0.070 m	Inside the core	**ULTEM***	2/10
2	0.070 m	Inside the core	**Iron**	2/10
2	0.070 m	**Inside the core**	Iron	2/10
3	0.070 m	**Outside the core**	Iron	2/10
3	**0.070 m**	Outside the core	Iron	2/10
4	**0.173 m**	Outside the core	Iron	2/10
4	0.173 m	Outside the core	Iron	**2/10**
5	0.173 m	Outside the core	Iron	**4/20**

* high-performance thermoplastic polymer.

2.1 FEM simulations and results

The torque acting on each ring was evaluated for each case by rotating the outer ring and assessing the torque at each position. Figure 2a shows the torque in Nm experienced by the rings as a function of the rotational angle of the outer rotor for the model with a radius of 0.070 m using ULTEM material (*id* value equal to 1 in Table 1). Figure 2b presents the torque for a ferrous material with the same outer radius and magnet position (*id* value equal to 2 in Table in Figure 2a and Figure 2b. From Figures 2a and 2b, it can be observed that the torque behavior is periodic with a mean of zero for all three rings. This is due to the relative positions of the

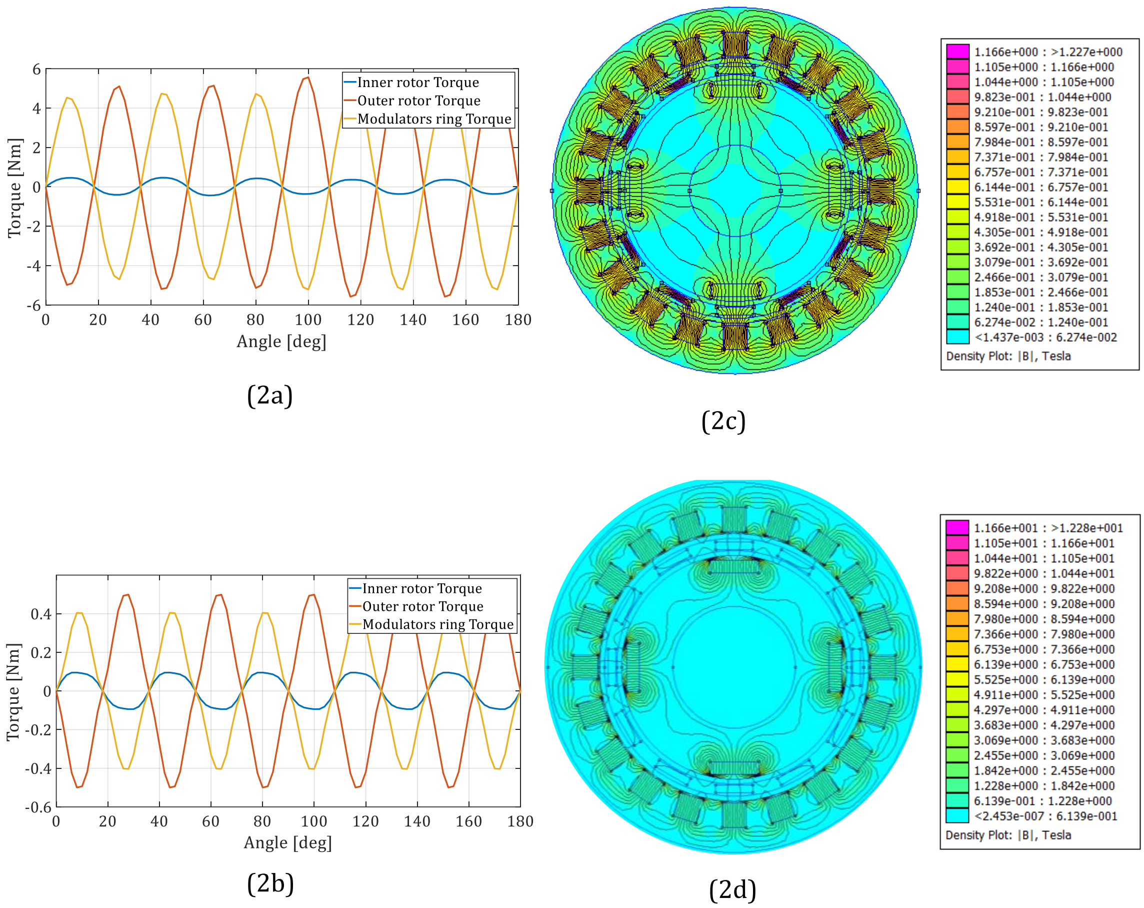

Figure 2. (a) Torque profile in Newton-meters (Nm) as a function of the angular position of the outer ring in degrees for rings made of ULTEM, with an outer radius of 0.070 m; (b) Torque profile in Newton-meters (Nm) as a function of the angular position of the outer ring in degrees for rings made of iron, with an outer radius of 0.070 m; (c) Magnetic flux behavior for the ULTEM model and colour map from cyan (1,437 x 10^{-3}T÷6.274x10^{-2}T) to purple (1,166 T ÷ >1,227 T); (d) Magnetic flux behavior for the iron model and colour map from cyan (1,437 x 10^{-3}T÷6.274x10^{-2}T) to purple (1,166 T ÷ >1,228e+001 T).

magnets and modulators as the angular position of the outer rotor varies, and the fact that the outer ring is the only movable element in the system. All trends reach a maximum or a minimum for the same angle value, and in accordance with equation (1), the torque induced on the inner rotor is out of phase with that on the outer rotor, while it is in phase with the torque induced on the modulator ring1). Figure 2c and Figure 2d depict the magnetic flux behavior, with a colour map indicating the density of magnetic flux expressed in Tesla (T), respectively for the simulation cases presented.

More, Figures 2a and 2b illustrate the magnitude of inducted torque on the rings with magnets and modulators due solely to their immersion in a rotating magnetic field. In both scenarios, the highest torque peak is observed in the outer ring. However, there is an order of magnitude difference in the perceived torque between case 2a and case 2b, with values reaching 5.5 Nm in the former and 0.45 Nm in the latter. Notably, despite ULTEM having a magnetic permeability comparable to that of air—which is negligible especially in comparison to iron—it seemingly achieves better results than the iron rings. To elucidate this outcome, reference is made to Figure 2c-d. In Figure 2c, it is observed that the magnetic flux lines tend to disperse within the ring, involving a loss factor. Specifically, many flux lines in proximity to the outer rotor do not close, indicating substantial losses in the system. In addition, according to the colour map, the density of magnetic flux on the modulators and on the outer ring magnets is very high. It involves an overheating of the parts and the de-magnetization of outer rotor pole pairs, hence more losses. Conversely, Figure 2d shows several lines of magnetic flux close the magnets, particularly in the inner rotor. Here the flux becomes trapped within the core, preventing interaction with the modulators and magnets in the outer rotor and resulting in heating of the core and magnets. About the flux density, it appears weak in all regions, except at the edges of the outer and inner rotor.

Figures 3a and 3b report the results of the configuration with id 3 in Table 1. They respectively illustrate the torque acting on the rotors in Newton-meters (Nm) as a function of the angular position of the outer ring, and the behavior of the magnetic flux lines when the magnets are no longer embedded within the ferrous core, and the correspondent colour map for magnetic flux density identification.

From Figure 3a, it is observed that the torque experienced by the rings has increased by two orders of magnitude compared to the case with magnets placed inside the ferrous core passing from 0.4 to 15 Nm. Additionally, it is evident that the torque in the modulator ring is higher in this configuration, reaching an absolute value of 10 Nm, compared to 7.5 Nm for the outer ring. Figure 3b shows the behavior of the magnetic flux lines for the same configuration. It highlights that the magnetic flux lines tend to move towards the modulators and subsequently interact with the external magnets. In the vicinity of these external magnets, an increase in magnetic flux density is observed. As in the previous case, this may lead to material saturation, rendering it diamagnetic.

Figures 4a and 4b, respectively, present the torques acting on the rotors as a function of the angular position of the outer rotor and the magnetic flux distribution for the model with an outer radius of 0.173 m and external magnet placement (so the id configuration value is equal to

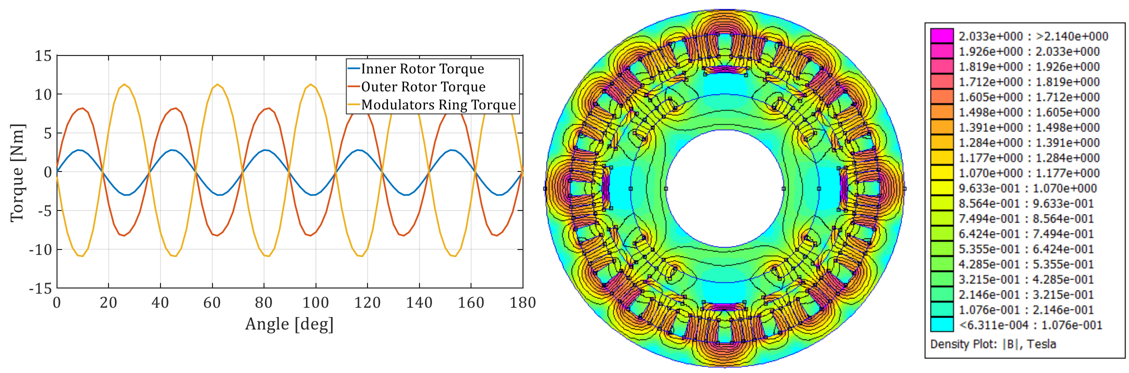

(3a) (3b)

Figure 3. (a) Torque profile in Newton-meters (Nm) as a function of the angular position of the outer ring in degrees for iron rings with an outer radius of 0.070 m and magnets positioned outside the core; (b) Magnetic flux behavior for the iron model with external magnets and the correspondent magnetic flux density colour map.

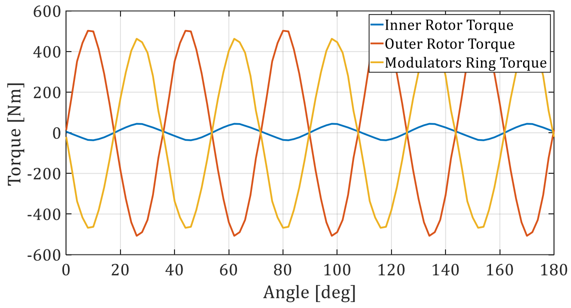

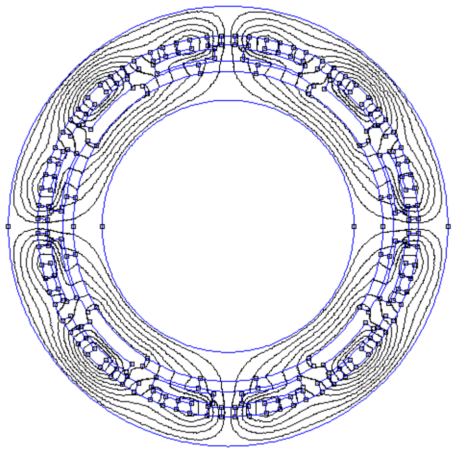

(4a) (4b)

Figure 4. (a) Torque profile in Newton-meters (Nm) as a function of the angular position of the outer ring in degrees for iron rings with an outer radius of 0.173 m and magnets placed outside the core; (b) Magnetic flux distribution for the iron model with external magnets and an outer radius of 0.173 m.

4 in Table 1). Due to the larger size of the model mesh—over 120000 triangles and 60000 nodes — the software couldn't generate a complete map for the magnetic flux density evaluation.

Increasing the outer radius results in a proportional increase in the spacing angle of the magnets and modulators, as their dimensions have been scaled accordingly.

From Figure 4a, it is evident that the torques involved are significantly high, with the modulator ring achieving a maximum absolute value of 507 Nm. Figure 4b shows a more optimal distribution of the magnetic flux, primarily due to a slight increase in the size of the magnets on the inner rotor. However, this distribution could be further improved by increasing the thickness of the ring to allow the flux to occupy a larger space, although this would also increase the weight.

Figures 5a and 5b respectively illustrate the torque acting on the rotors and the magnetic flux distribution for a model with the same characteristics as the previous one, except for the number of pole pairs on the inner and outer rotors, which are 4 and 20, respectively, maintaining a 1:5 ratio that represent the configuration with an *id* value of 5.

Figure 5a shows that increasing the number of pole pairs not only enhances the torque in absolute terms, reaching approximately 835 Nm for the modulator ring, but also increases the oscillation frequency by 100% due to the presence of additional magnets.

Figure 5b presents the magnetic flux distribution for the new system configuration.

3. Discussion and conclusions

This study presents a comprehensive energy efficiency comparison of various concentric magnetic gearbox configurations, with a focus on torque performance. Utilizing two-dimensional Finite Element Method (FEM) simulations, different configurations have been analyzed, varying geometrically and technologically. The comparison covered unloaded conditions and variations in four key parameters: outer ring radius, ring material, magnet placement, and the number of magnets, while maintaining a consistent transmission ratio. Details are provided in Table 1.

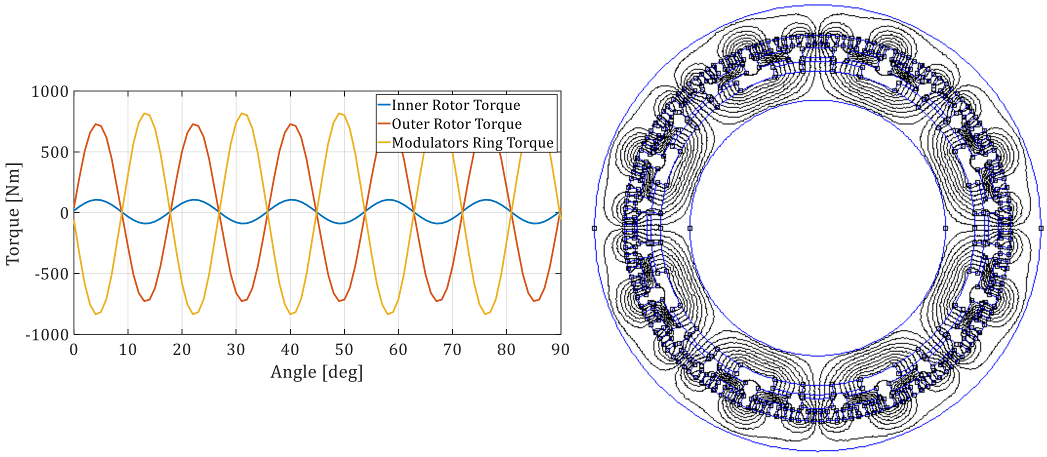

(5a) (5b)

Figure 5. (a) Torque variation in Newton-meters (Nm) as a function of the angular position of the outer ring in degrees for iron rings with an outer radius of 0.173 m, magnets positioned outside the core, and with p_i=4 and p_o=20; (b) Magnetic flux variation for the iron model with external magnets, an outer radius of 0.173 m, and with p_i=4 and p_o=20.

Our findings indicate that using ULTEM, a polymer with high thermal resistance but low magnetic permeability, as a core material for housing permanent magnets is not ideal. Although initially appearing advantageous over an iron core, the ULTEM model offers limited torque improvement and suffers from significant magnetic flux leakage, leading to low efficiency and high dispersion losses.

Magnet placement is also critical. When magnets are embedded within the ferrous core, flux lines become confined, creating a loss factor as the flux closes internally rather than linking externally. Conversely, positioning magnets on the core's surface (radius 0.070 m) allows the modulator ring to reach a peak torque of 11.5 Nm, compared to 0.5 Nm with internal magnets.

Additionally, increasing the gearbox size proportionally enlarges the angle spanned by the magnets, leading to a significant rise in induced torque, up to 507 Nm with the modulator ring. The number of pole pairs, with the same transmission ratio, plays a crucial role in enhancing torque due to constructive magnet interactions, also increasing oscillation frequency by 100%. This frequency increase is vital for system stability under load and with multiple rotating rings, ensuring a non-zero average torque.

In summary, while the ULTEM-based configuration shows some potential, the ferrous core with external magnets significantly outperforms it in torque and efficiency. These results underscore the importance of optimizing both material choice and magnet placement to enhance concentric magnetic gearbox performance.

References

[1] Vargas S A, Esteves G R T, Maçaira P M, Bastos B Q, Cyrino Oliveira F L and Souza R C 2019 Journal of Cleaner Production 218 850-70

[2] González M O A, Gonçalves J S and Vasconcelos R M 2017 Journal of Cleaner Production 142 461-75

[3] Tummala A, Velamati R K, Sinha D K, Indraja V and Krishna V H 2016 Renewable and Sustainable Energy Reviews 56 1351-71
[4] Bharani R and Sivaprakasam A 2022 IETE Journal of Research 68 3341-55
[5] Bhardwaj U, Teixeira A P and Soares C G, Renewable Energy 141 693-706
[6] Su C, Yang Y, Wang X and Hu Z 2016 Prognostics and System Health Management Conference (PHM-Chengdu) 1-6
[7] Salameh J P, Cauet S, Etien E, Sakout A and Rambault L 2018 Mechanical Systems and Signal Processing 111 251-64
[8] Al-Bahadly I, 2011 Wind Turbine (Intech Open)
[9] Liu W Y, Tang B P, Han J G, Lu X N, Hu N N and He Z Z 2015 Renewable and Sustainable Energy Reviews 44 466-72
[10] Jian L, Chau K T and Jiang J Z 2009 IEEE Transactions on Industry Applications 45 954-62
[11] Chau K T, Zhang D, Jiang J Z, Liu C and Zhang Y IEEE Transactions on Magnetics 43 2504-06
[12] Atallah K, Claverley S D and Howe D 2004 IEE Proceedings - Electric Power Applications 135
[13] Rasmussen P O, Andersen T O, Joergensen F T and Nielsen O 2003 38th IAS Annual Meeting on Conference Record of the Industry Applications Conference 1696-702
[14] Tlali P M, Wang R-J and Gerber S 2014 International Conference on Electrical Machines (ICEM) 544-550
[15] Atallah K and Howe D 2001 IEEE Transactions on Magnetics 37 2844-46
[16] A. Amoresano, L. P. Di Noia, R. Rizzo, e S. Roscioli, *2023 International Conference on Clean Electrical Power (ICCEP)*, Terrasini, Italy: IEEE, giu. 2023, pp. 735–739. doi: 10.1109/ICCEP57914.2023.10247396.